



Contents lists available at ScienceDirect

Arabian Journal of Chemistry

journal homepage: www.ksu.edu.sa

Antimicrobial attributes and enhanced catalytic potential of PVA stabilized Ag-NiO₂ nanocomposite for wastewater treatment

Aimon Saleem^a, Amber Iqbal^a, Umer Younas^{a,*}, Adnan Ashraf^a, Samiah H. Al-Mijalli^{b,*}, Faisal Ali^{a,*}, Muhammad Pervaiz^{c,*}, Zohaib Saeed^c, Arif Nazir^a, Munawar Iqbal^d

^a Department of Chemistry, The University of Lahore, Lahore, Pakistan

^b Department of Biology, College of Sciences, Princess Nourah bint Abdulrahman University, P.O. Box 84428, Riyadh 11671, Saudi Arabia

^c Department of Chemistry, Government College University Lahore, Lahore, Pakistan

^d Department of Chemistry, Division of Science and Technology, University of Education Lahore, Lahore, Pakistan

ARTICLE INFO

Keywords:

Dye degradation
Antimicrobial activity
Silver-nickel
Nanocomposite
pH studies

ABSTRACT

Dyes are well known major pollutants in wastewater discharged by various textile industries which are toxic to human beings and aquatic life. It is necessary to remove these colorants from water with low-cost yet effective method by which these pollutants can be removed from the water bodies. Current study has been designed to develop cost-effective material for the removal of dyes in wastewater along with the application of composite to inhibit the growth of Gram negative (GN) and Gram positive (GP) bacterium. Nanocomposite (Ag-NiO₂@PVA) of silver and nickel was synthesized by the chemical reduction method and polyvinyl alcohol (PVA) was used as a stabilizing medium. Nanocomposite (NC) was characterized employing different techniques including XRD, SEM, and FTIR which not only confirmed its synthesis but also provided their structure and morphology. The hexagonal close packed nanocomposite was tested for the catalytic degradation of different azo and anthraquinone dyes including methylene blue (MB), methyl orange (MO) and eosin yellow (EY). The degradation of MO, MB and EY was recorded in 20, 16 and 20 min with percentage removal 89.26, 95.88 and 96.56 % respectively. Antibacterial potential of the nanocomposite was assessed against different GN and GP bacterial strains namely *Bacillus subtilis*, *Staphylococcus aureus* and *Escherichia coli* and the as-synthesized Ag-NiO₂@PVA exhibited strong zone of inhibition against all types of bacterial strains mentioned herein. Nanocomposite was recovered and analyzed after dye degradation as well as the antibacterial studies have confirmed stability and recyclability of the nanocomposite. Results of the current study strongly recommend the composite for wastewater treatment applications i.e., removal of different dyes and pathogens. Silver and nickel based nanocomposite can be synthesized and modified followed by the stabilization with PVA for different applications in material sciences.

1. Introduction

The most current and broiling topic of research around the globe is the treatment of water as contamination is increasing quite drastically due to urbanization and industrialization (Benkhaya et al., 2020). Owing to many anthropogenic activities, it has now become quite difficult to get pure water for domestic and for drinking purposes (Moustakas, 2021). The major water pollutants reported in contaminated water are nitro-arenes (Tokawa et al., 1986, Singh et al., 2022), heavy metal ions (Li et al., 2019), pesticides and noxious dyes (Muenze

et al., 2017). Organic dyes such as azo (AZ) and anthraquinone (AQ) dyes stand out as the key component of the wastewater due to their vast industrial applications (Shindy, 2017, Vacchi et al., 2017). These dyes are consumed in paper (as printing inks), pharmaceuticals (Chung, 2016), paints, lacquer, varnish and wood industries (Nitu et al., 2022). AZ and AQ are also being used for dyeing natural and synthetic textile fibers, leather and plastics (Bide, 2014). These dyes are versatile and largest class of colorants that account for more than 50 percent of the dyestuff produced globally (Puvanewari et al., 2006). As pollutants, these compounds are most stable and toxic; for this reason, most of the

Peer review under responsibility of King Saud University.

* Corresponding authors.

E-mail addresses: umer0608analyst@gmail.com (U. Younas), Shalmejale@pnu.edu.sa (S.H. Al-Mijalli), faisal.ali@chem.uol.edu.pk (F. Ali), dr.mpbhatti@gcu.edu.pk (M. Pervaiz).

<https://doi.org/10.1016/j.arabjc.2023.105545>

Received 27 September 2023; Accepted 7 December 2023

Available online 9 December 2023

1878-5352/© 2023 The Author(s). Published by Elsevier B.V. on behalf of King Saud University. This is an open access article under the CC BY license (<http://creativecommons.org/licenses/by/4.0/>).

Table 1
Conditions for the catalytic degradation of dyes.

Sr. No.	Dyes	Concentration of dye used in mM	Concentration of Reducing agent used in mM	Concentration of catalyst used mg/mL
1	MB	1.6 mL of 0.02 mM	0.5 mL of 2 mM	0.05 mg/mL
2	MO	1.6 mL of 0.01 mM	0.5 mL of 1 mM	0.05 mg/mL
3	EY	1.6 mL of 0.04 mM	0.5 mL of 4.6 mM	0.05 mg/mL

countries have banned their use due to their detrimental effects on the human as well as the aquatic life (Ahlström et al., 2005). In developing countries, dyes belonging to the aforementioned class are still in use. Almost 10% of the total amount of dyes used in dyeing procedure, becomes the part of wastewater (Manzoor and Sharma, 2020). The World Health Organization (WHO) has projected the contribution of AQ and AZ in the water pollution to be around 17 – 20% as compare to all the other pollutants emerging from different industries (Sarkar et al., 2017). Due to their detrimental effects, it is necessary to investigate and design, cost-effective and facile methods to eliminate dyestuff from wastewater. Efforts have been made and researchers have reported different materials such as polymers, microgels (Shahid et al., 2020), monometallic nanoparticles (MNPs)/ bimetallic nanoparticles (BMNPs) (Shultz et al., 2019), metal–organic-frameworks (Liu et al., 2020) and metal nanoparticles loaded in hydrogels (Arif et al., 2021) for the removal of dyes from aqueous streams. Despite many conventional methodologies

including forward and reverse osmosis, adsorption, multi-effect and membrane distillation; photocatalysis have been extensively developed for the treatment of wastewater. Researchers are still struggling to develop novel, sustainable and cost-effective procedures for the treatment of dye carrying wastewater (Noureen et al., 2021).

The MNPs/BMNPs have gained attention due to their recyclability and high catalytic efficacy (Mallampati and Valiyaveetil, 2014) but their instability have been an issue which can be controlled by the usage of polymers, surfactants (Song et al., 2021), microgels and dendrimers (Shahid et al., 2022). In comparison to pure MNPs, BMNPs, nanocomposites (NCs) exhibit extraordinary optical, catalytic and electronic properties because of their improved phase coupling. There are many methods including co-precipitation (Bakar et al., 2009), sol–gel (Lamayi et al., 2020), micro-emulsion (Heshmatpour et al., 2012), wet-chemical (Ould-Ely et al., 2005), solvothermal (Bondesgaard et al., 2019) and hydrothermal (Shen et al., 2017) that have been reportedly used for the synthesis of BMNPs and heterogeneous/mixed NCs (Ullah et al., 2023). The chemical reduction method is preferred because of its mild reaction conditions, lower energy consumption, simple separation procedures, reproducibility and high yield (Liu et al., 2010).

In recent studies, p-type semiconducting materials specially transition metals oxides (NiO_2 , FeO , Cu_2O) are being used for the catalytic degradation of different organic dyes (Bishnoi et al., 2018, Mrunal et al., 2019, Bhat et al., 2020). Transition metals, specially Nickel (Ni) based nanomaterials are considered to be the most effective for the

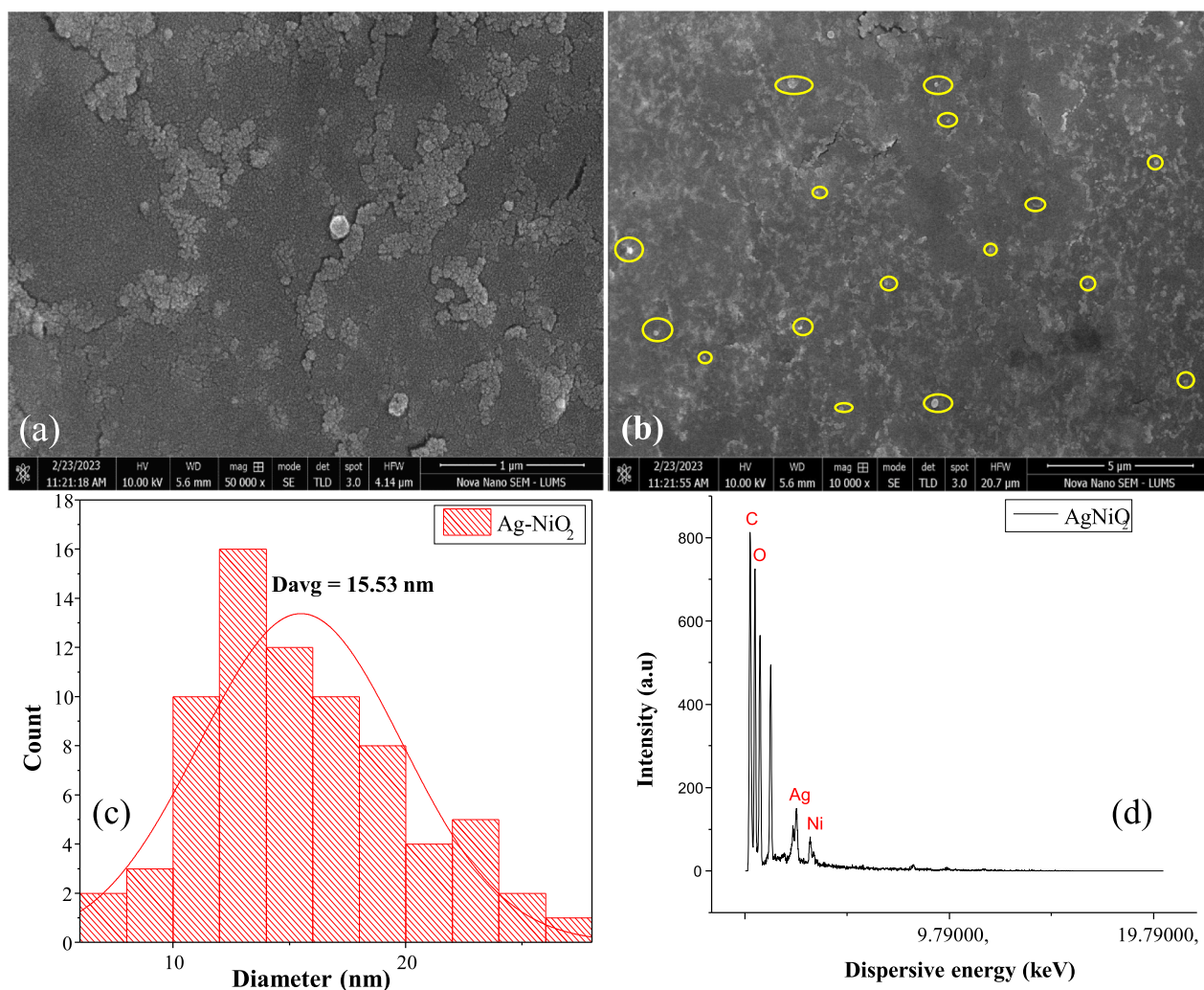


Fig. 1. (a-b) SEM images, (c) particle size distribution, (d) elemental analysis of the synthesized nanocomposite.

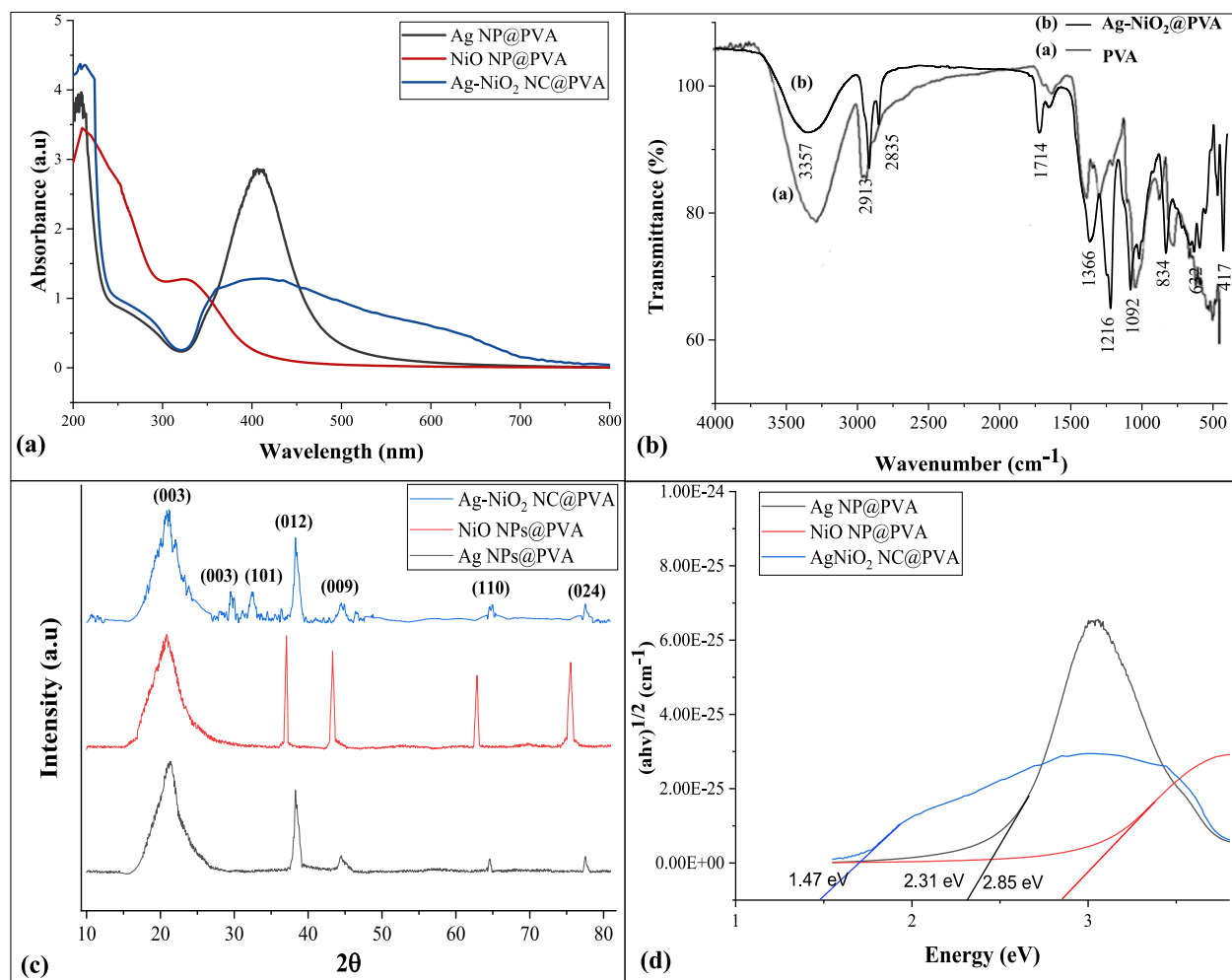


Fig. 2. (a) UV/Vis spectra, (b) FTIR spectra, (c) XRD analysis (d) Energy band gap of Ag-NiO₂@PVA NC.

degradation of dyes due to higher stability as well as antiferromagnetic and electrical properties (Sachi et al., 2021). Nickel peroxide nanoparticles (NiO₂ NPs) show a high opto-electric ability with a band gap of 3.6–4.0 eV (Khairnar and Shrivastava, 2019) and these NPs are extensively used in solar cells, gas/humidity sensing devices (Mokoena et al., 2019, Gupta et al., 2021), catalysis (Din et al., 2018) and electrochemical water splitting (He et al., 2021). Likewise, silver nanoparticles (Ag NPs) are now preferred as catalyst for dye degradation reactions due to its attractive morphology, larger surface to volume ratio and smaller size (Tang and Zheng, 2018). It is a well-established fact that the noble metals are the most suitable candidates for the degradation of dyes but there are two major problems associated to these materials: limitation of the catalyst, cost effectiveness and its recovery/ reusability. Therefore, fabrication of BMNPs and composites have surpassed the usage of traditional noble metal NPs (Wojtaszek et al., 2023). This results in improved catalytic activities that may be attributed to the prevailing synergistic-effect elevated by the development of interface-junction in the hetero-structures especially nanocomposites (Humayun et al., 2021).

In order to achieve promising results, nanomaterials have been modified and polymeric nanocomposites have gained attention due to improved properties which depends on the size distribution, geometry and surface chemistry (Kanchana and Vijayalakshmi, 2020). Although, the properties of NCs depends mainly on the nature of NPs and their ability to bridge physically and chemically with the matrix (polymer) (Yu et al., 2018). Amongst many other natural and synthetic polymers, poly vinyl alcohol (PVA) has excellent charge-storage capability (Wang

et al., 2021), greater dielectric strength and electric properties that are dopant dependent (Rashad, 2020). Suitable inorganic NPs can be incorporated to selected polymer to fabricate a material with desired properties and stability (Bouzidi et al., 2020).

In current study, a cost-effective and facile chemical reduction method has been employed for the synthesis of novel nanocomposite (Ag-NiO₂@PVA). Synthesis of Ag and Ni based bimetallic nanoparticles followed by stabilizing with PVA has been successfully achieved. To the best of our knowledge, PVA stabilized Ag-NiO₂ nanocomposite has never been synthesized by the aforementioned method and this combination has never been investigated for antimicrobial studies against different bacterial strains and evaluating the degradation of different dyes. Stability and reusability of the composite has also been checked and reported.

2. Experimental

2.1. Chemicals & reagents

Chemicals such as nickel sulfate hexahydrate (NiSO₄·6H₂O) (purity ≥ 99.9%), Silver nitrate (AgNO₃) (purity ≥ 99.9%), Sodium hydroxide (NaOH) (purity ≥ 99.5%), MB, EY, Sodium borohydride (NaBH₄), Sodium dodecyl Sulfate (SDS) (purity ≥ 99.0%), MO and Polyvinyl alcohol (PVA) with a density of 1.08 g/cm³ and the molecular weight of 89,000 – 98000 + 99% hydrolyzed were used as purchased from Sigma Aldrich, USA. Potassium persulfate (K₂S₂O₈), and potassium hydroxide (KOH) were purchased from Strem Chemicals, USA and were used as received.

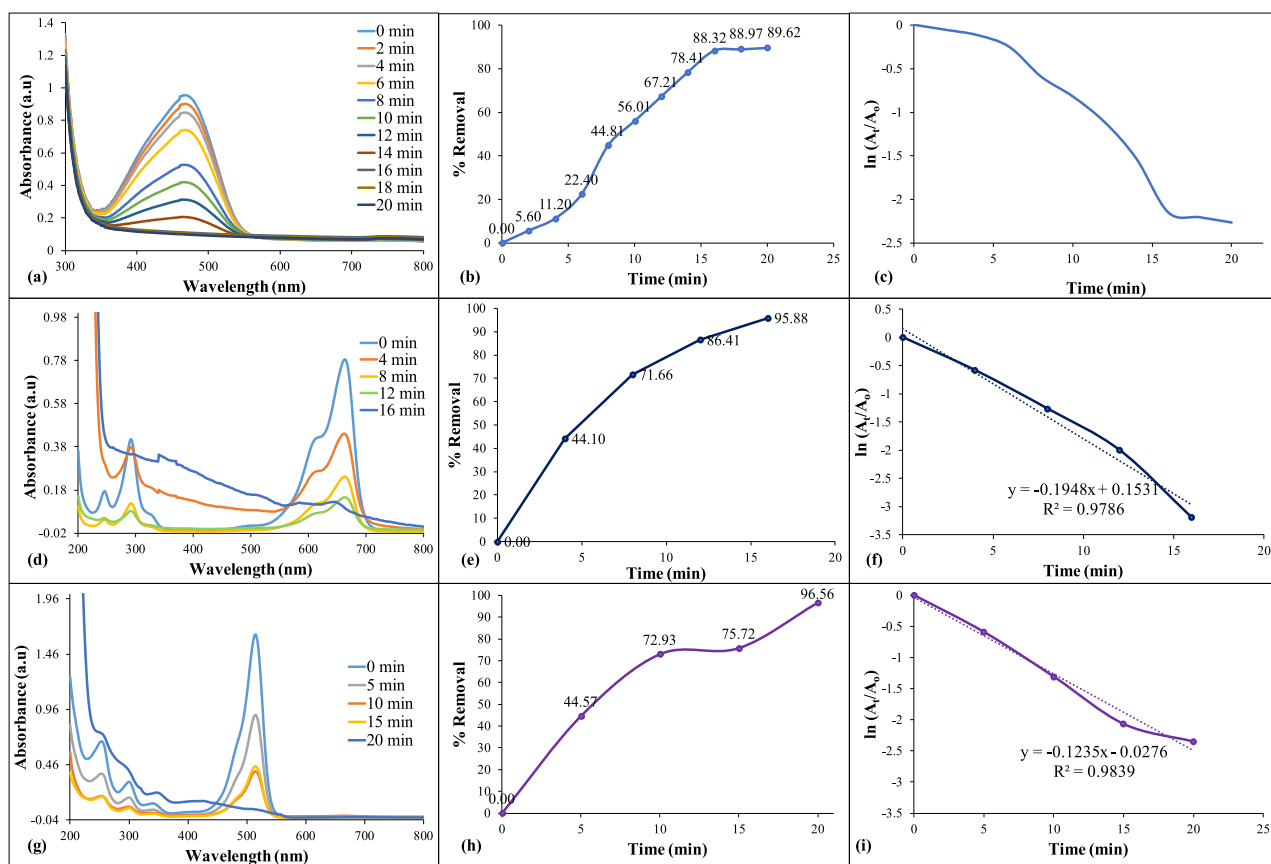


Fig. 3. (a, d, g) degradation of dyes, (b, e, h) % removal of dyes, (c, f, i) kinetic of degradation.

Deionized (DI) water was used throughout the experimental work.

2.2. Synthesis of the Ag-NiO₂@PVA nanocomposite

Nickel peroxide NPs (0.1 M) were synthesized following an already reported chemical reduction method (Shoair et al., 2023). Equi-molar NiSO₄·6H₂O and K₂S₂O₈ were taken in deionized water along with 0.1 g of PVA (50 mL DI) and stirring was done for 1 h at room temperature. The color of the solution turned black confirming the formation of NiO₂ NPs; then resultant mixture was filtered and washed thrice with deionized water in order to remove the unreacted salts and dried the sample for 3 h at 60 °C (Shoair et al., 2023).

Similarly, 0.1 g PVA was dissolved in 50 mL DI and was heated with continuous stirring for about 10 min at 60 °C in order to get a homogeneous solution. Then, silver nitrate solution (1 mL of 0.2 M) was added to the PVA solution followed by the addition of 0.2 mL of NaOH (0.3 M). The color of the solution immediately turned yellow right after the addition of base (NaOH); indicating the formation of Ag NPs (Sagitha et al., 2016).

For the synthesis of polymeric stabilized nanocomposite an already reported method (Khalil et al., 2021) was adopted with few modifications, 20 mL of DI was taken in a round bottom flask along with that 0.05 g SDS (surfactant) and 0.085 g of PVA were added in the same flask respectively. The mixture was kept on a magnetic hot plate for 1.5 h at 80 °C with continuous stirring. The reaction mixture was then taken off from the hot plate till the temperature drops down to 40 °C. At this point, 5 mL of as-prepared Ag NPs and 10 mL of NiO₂ NPs solutions were added with continuous stirring. After 5 min, 5 mL (0.05 M) NaBH₄ (reducing agent) was added drop wise to the reaction mixture until the color of the solution changes to pale yellow (Piella et al., 2017, Wojtaszek et al., 2023). This change in color was the visual confirmation of the NC synthesis.

2.3. Characterization of Ag-NiO₂@PVA nanocomposite

Synthesis of Ag-NiO₂@PVA NC was confirmed instantly after obtaining the liquid sample of the NC for UV/Vis analysis (CECIL, Model Aquarius CE 7400, CECIL, Cambridge, U.K.). Remaining NC mixture was centrifuged for 30 min at 11,000 and FTIR analysis of the solid sample was done using FTIR, Model Alpha (II), Bruker, U.K. respectively. The morphological and elemental analysis was investigated using Field emission-scanning electron microscopy (FE-SEM, Model NOVA FE-SEM 450) coupled with energy-dispersive X-ray analysis (EDAX). Crystalline examination was performed by the XRD analysis (Bruker, Coventry, U. K.).

2.4. Catalytic degradation potential of Ag-NiO₂@PVA nanocomposite

The degradation potential of the synthesized NC (Ag-NiO₂@PVA) was investigated against three different dyes (MO, MB, EY). The optimized condition (Table 1) recorded for the degradation of MB was; 1.6 mL of 0.02 mM MB dye, NaBH₄ (0.5 mL of 2 mM) and 0.05 mg/mL NC were taken into the reaction cuvette for the monitoring of dyestuff degradation. Correspondingly, 1.6 mL of 0.01 mM MO, 0.5 mL of 1 mM NaBH₄ and 0.05 mg/mL NC were the optimum condition used for the degradation of MO dyestuff. Similarly, the optimal ratios of EY dye were having molarity of 0.04 mM EY, 4.6 mM NaBH₄ and 0.05 mg/mL of NC (Piella et al., 2017, Ali et al., 2023). Absorption spectra of the resultant mixtures were recorded after regular time intervals by UV/Vis spectrophotometer. Percentage degradation was calculated by the formulae % degradation = $(C_i - C_t)/C_i \times 100$; where C_i is the initial concentration of the solutions of dye's taken and C_t is the specific time concentration (Baz et al., 2023). As the pH of the medium plays an important role in the catalytic removal of different dyes (Lai et al., 2019). These catalytic experiments were also performed at room temperature and maintaining

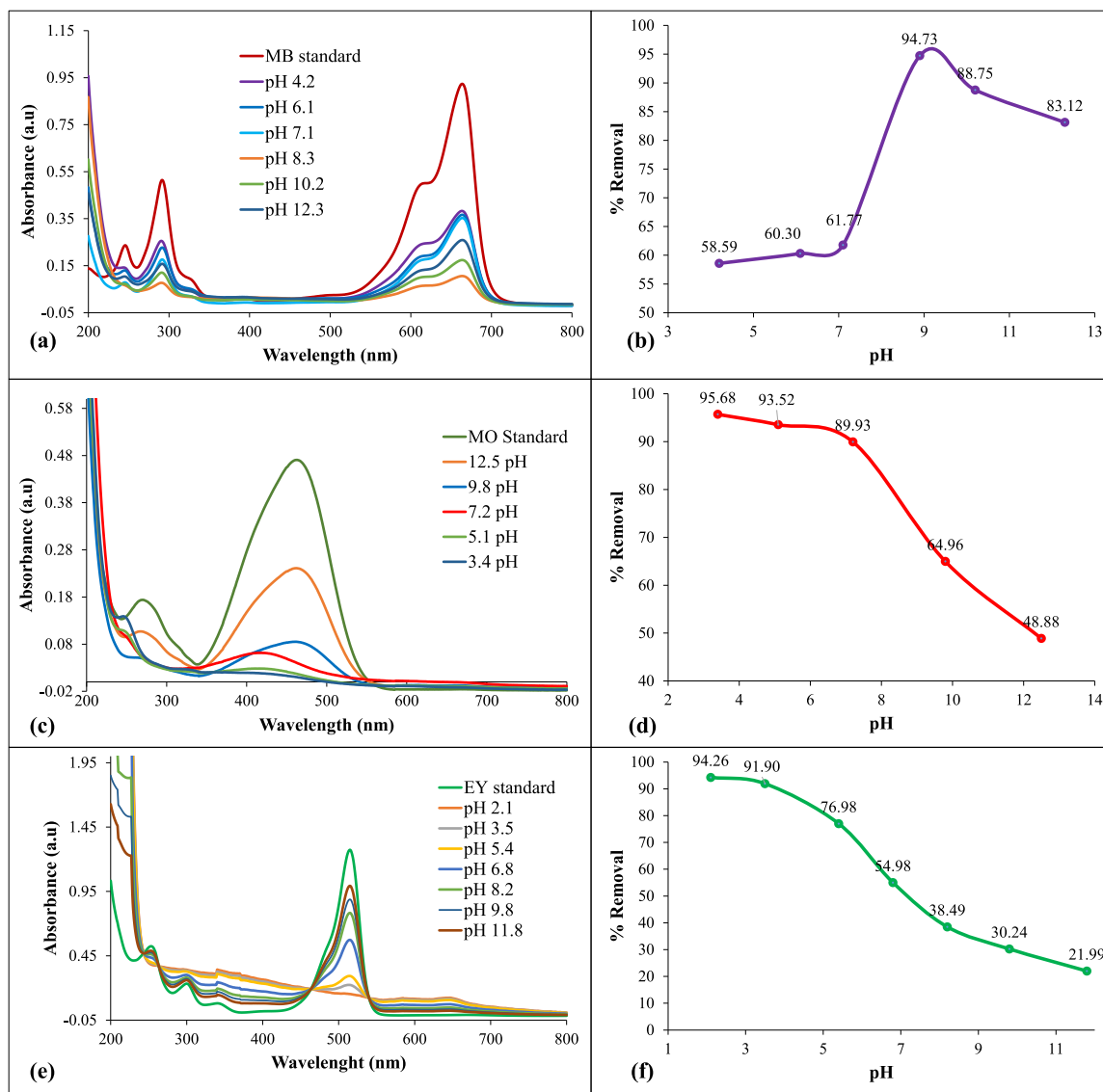


Fig. 4. Impact of pH on (a) MB degradation, (b) % removal (c) MO degradation, (d) % removal (e) EY degradation, (f) % removal.

different pH conditions basic (0.1 M NaOH) and acidic (0.1 M HCl) (Ali et al., 2023). Reusability of the NC was evaluated by carrying out four cycles of MB dye degradation reaction. Percentage degradation was calculated followed by FTIR analysis of recovered NC after completion each cycle of MB degradation reaction.

2.5. Antimicrobial studies of Ag-NiO₂@PVA

The as-synthesized NC was tested against Gram positive (*Staphylococcus aureus* NCTC 7447) and Gram negative (*Bacillus subtilis* NCIB 3610) and *Escherichia coli* NCTC10416) bacterial strains to evaluate antimicrobial potential using disc diffusion method (DDM) (Ali et al., 2022). The mixture containing nutrient broth and agar-agar media were autoclaved for 20 min at 121 °C. Then, 30 mL sterilized medium was poured down into petri-dishes using laminar flow cabinet. The strains carrying disc were transferred to petri dish and upon solidification, 30 µL of the sample was wedged onto the discs using micropipette. The petri dish was imperiled to incubation at 37 °C for 24 h. The zone of inhibition (ZOI) was calculated in mm. Penicillin was taken as a positive control while DMSO as a negative one, respectively for the antibacterial activity.

3. Results and discussion

3.1. Surface morphology and elemental analysis

The elemental analysis and morphology of the synthesized NC has been investigated using Field Emission Scanning Electron Microscope (FESEM) and EDAX. The images of Ag-NiO₂@PVA NC are shown in Fig. 1(a, b). The elemental composition of Ag-NiO₂@PVA was experiential by EDAX analysis as presented in Fig. 1d that also measures elemental distribution in order to find out any possible interfacial interaction. The average particle size calculated from SEM images is 15.53 nm and the particles are distributed in between the ranges 0–30 nm and the particle size distribution has been presented in Fig. 1c. SEM images have shown homogeneous pattern throughout with the spherical-nanospheres of Ag-NiO₂ stabilized by PVA and SDS; same nature of particles has been reported in previous studies (Sagitha et al., 2016, Karunamoorthy and Velluchamy, 2018).

3.2. UV/Vis analysis of Ag-NiO₂@PVA composite

Fabrication of Ag-NPs, NiO₂-NPs, and Ag-NiO₂@PVA NC was

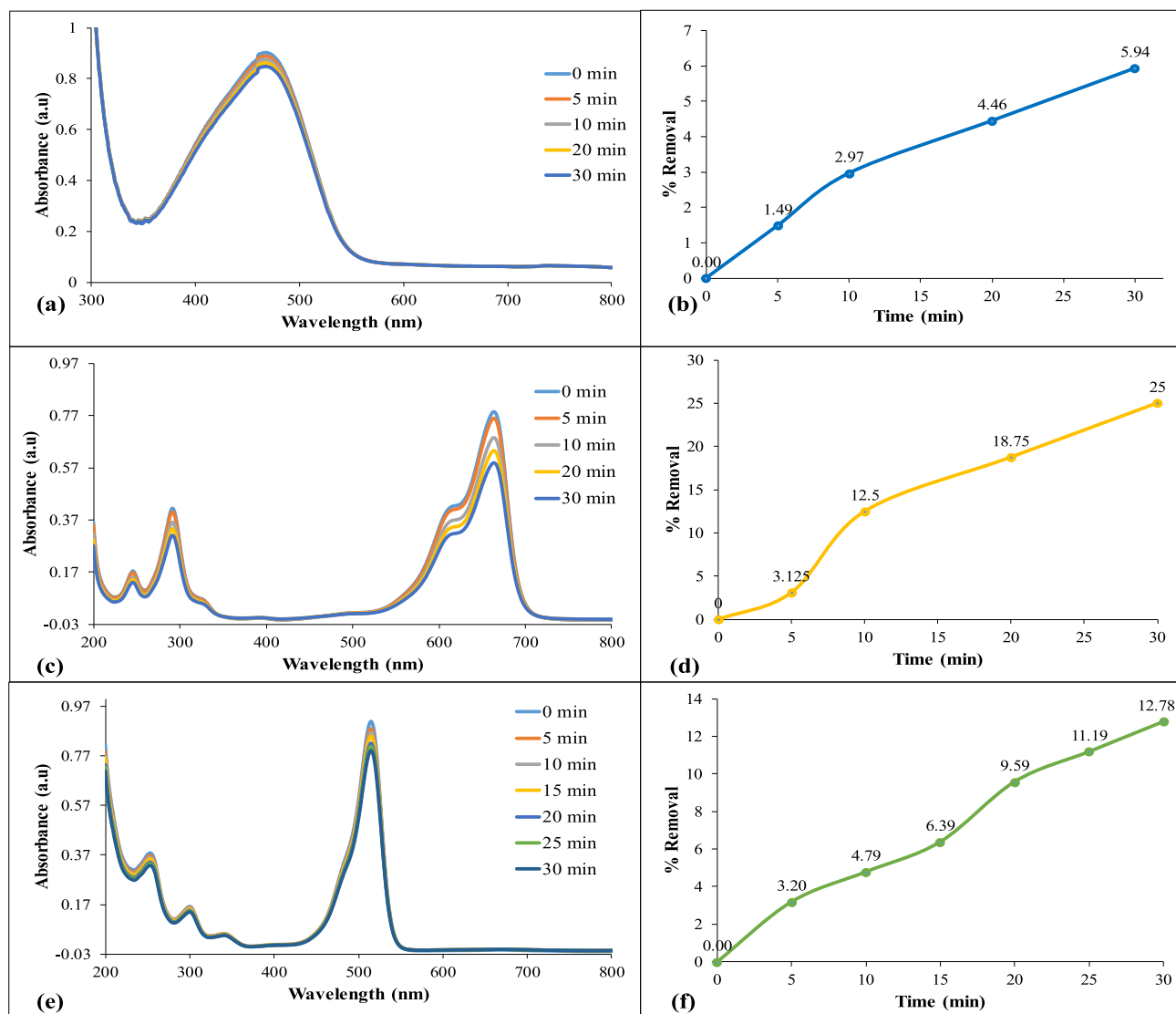


Fig. 5. (a-b) UV/Vis Spectra of controlled reaction of MO, (c-d) MB, and (e-f) EY in the absence of Ag-NiO₂@PVA.

confirmed by the UV/Visible analysis and the spectrum recorded is shown in Fig. 2(a). Results indicated λ_{max} of Ag at 452 nm which bear a resemblance to the previously reported work (Ali et al., 2023) and that of NiO₂ at 300 nm are analogous to the ones already reported (Shoair et al., 2023). The immense shift in λ_{max} is due to the interference of Ag's λ_{SPR} . The broad nature of the band at some regions could be due to the presence of polymer in the solution as the clear broader peaks have been observed for the NC which explains the nature of both the metals and polymer's interaction as explained by (Arif, 2023) in his work. The energy band gap (EB) was found using Tauc plot (Fig. 2d). The results revealed that AgNPs@PVA exhibit EB at 2.31 eV, NiONPs@PVA have shown EB at 2.85 eV, whereas Ag-NiO₂@PVA NC has shown exceptional EB value at 1.47 eV. This lowering in EB may be due to the presence of the amalgamation of Ag and NiO₂ with PVA.

3.3. FTIR analysis of Ag-NiO₂@PVA

FTIR spectroscopic analysis of the fabricated nanocomposite and PVA has been presented in Fig. 2b. Peaks in the ranges between 500 and 550 cm⁻¹ in Fig. 2b (b) can be allotted to NiO stretching which are closely resembled to already reported peaks (Kooti and Jorfi, 2009, Teoh and Li, 2012). The feeble absorption band at 710 cm⁻¹ is a distinctive (O-O) per-oxo stretching vibrational peak (Li and Kawi, 1998) and the

peaks at 1001 and 1092 cm⁻¹ indicated the presence of S=O functional group in the surfactant (SDS). Dip appearing at 1366 cm⁻¹ shows the existence of asymmetric stretching of SO₃⁻. Similarly, peak at 1216 cm⁻¹ can be designated to the C-O stretching (Safajou et al., 2017) and a peak at 3357 cm⁻¹ described the alcoholic group in the polymeric matrix and is designated to O-H stretching (Kayal and Ramanujan, 2010). It was noticed that two weak bands at 2913 cm⁻¹ and 1714 cm⁻¹ respectively may be attributed to the O-H bending and H-O-H stretching vibrational modes (Ichyanagi et al., 2003). These peaks probably aroused due to the hydration in the sample disk while preparing the sample in open air (Shoair et al., 2023). These results were comparable to the ones reported previously in the literature. FTIR spectrum of the NC was compared with pure PVA presented as Fig. 2b (a); the intensity of the band (3360 to 3357 cm⁻¹) involving H-bonding in PVA was reduced after the conjugation with nanoparticles. The blue shift of the band at 2913 cm⁻¹ for CH₂ asymmetric stretching, validates the formation of H-bonds between NC and PVA chains. Disappearance of a dip at 1670 cm⁻¹ along with the reduction in the band's intensity from 1740 to 1714 cm⁻¹ and from 852 to 830 cm⁻¹ indicate the formation of chemical interactions amongst the NC and PVA (Mahmoud, 2015).

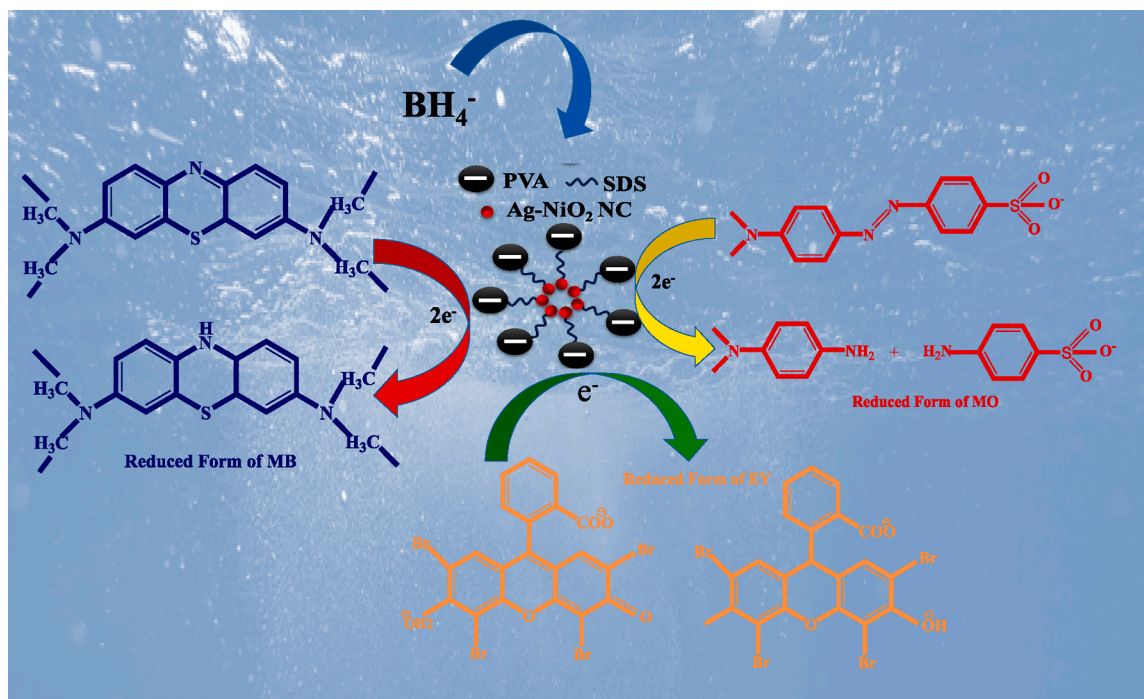


Fig. 6. Possible mechanism of catalytic degradation of dyes by Ag-NiO₂@PVA.

Table 2

Comparison between previously reported studies and present work.

Sr. No	Nano-catalyst	Dye	Reducing agent	% degradation	Reaction time	Ref.
1	Ag-NiO ₂ @PVA	MO	NaBH ₄	89.26	20 min	Present work
		MB		95.88	16 min	
		EY		96.56	20 min	
2	Ag-Ni NPs	MO	Photocatalysis	91	80 min	(Shaheen et al., 2020)
3	TiO ₂ -NiO-Ag	MB	Photocatalysis	93.8	90 min	(Sabzehparvar et al., 2021)
4	Ternary NiO/Ag/TiO ₂	MB	Photocatalysis	93.15	60 min	(Mohammed et al., 2023)
5	Ag/NiO	RhB	NaBH ₄	99.2	5 min	(Bhatia and Nath, 2022)
		Congo-R		95	6 min	
		MO		97.5	10 min	
		MB		98.3	10 min	
6	Ag@NiO composite	4-nitrophenol	NaBH ₄	90	65 min	(Sun et al., 2022)

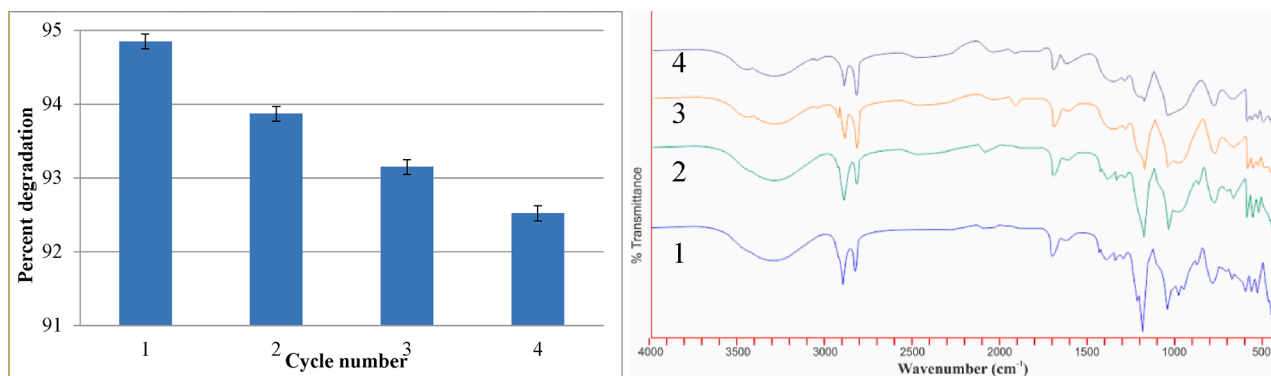


Fig. 7. (a) MB degradation potential of NC over the course of 4 cycles, (b) FTIR spectra for NC recovered during 4 cycles.

3.4. XRD analysis of Ag-NiO₂@PVA

The results of XRD analysis Ag NPs, NiO NPs, and Ag-NiO₂@PVA NC are shown in Fig. 2(c). The peaks at (1 1 0), (0 2 1), (1 0 1), (0 0 6), (0 0 9), (1 1 6) and (2 0 2) are in agreement with hexagonal close packing phase and the composite belongs to the JCPDS card No. 82-0007. The pattern

showed no additional peak which confirms the formation of single-phase of NiO₂ (Baz et al., 2023). Average crystallite size of Ag-NiO₂@PVA was 9.0145 nm. The peaks at 29.14°, 35.58°, 36.60°, 44.34°, 63.22° and 77.81° have been used to evaluate the crystallite size (D). The crystallite size (D) is calculated by the formulae: $D = 0.9 \lambda / \beta \cos \theta$ where wavelength is λ , β is FWHM in radian and θ is the Bragg's angle.

Table 3
Antibacterial activity potential of nanocomposite.

Material/ Control	<i>Bacillus subtilis</i> (+)	<i>Escherichia coli</i> (-)	<i>Staphylococcus aureus</i> (+)
AgNPs@PVA	7.5 mm	12 mm	10.75 mm
NiO ₂ @PVA	6.15 mm	10 mm	9.75 mm
Ag-NiO ₂ @PVA	9 mm	17.5 mm	15.25 mm
Penicillin (+)	3.25 mm	8.5 mm	4 mm
control			
DMSO (-) control	No activity	3 mm	1.85 mm

3.5. Dye degradation studies using Ag-NiO₂@PVA

Results of characterization confirmed the fabrication of nanocomposite via chemical reduction method and the NC was then tested for the catalytic removal of dyes (MB, MO and EY).

3.5.1. Removal of MO, MB, and EY dyes

Removal of the dyes was attained by achieving their degradation using NaBH₄ as reducing agent and synthesized NC as catalyst. An absorption peak is observed at λ_{\max} (464 nm) for MO indicating –N=N– group in the visible region the spectrum. Fig. 3a represents the degradation of the MO dye with a decrease in the peak till it becomes analogous to the abscissa for colorless solution in 20 min with the maximum percentage degradation up to 89.26% (Fig. 3b), which corresponds to the breakdown of the two aromatic rings of the AZ group present in MO. As a result of degradation, two products such as *N,N*-dimethylbenzenamine and sulfanilic acid were formed which gets converted into water and CO₂ (Xie et al., 2016).

MB has two different forms, one is an oxidized form having solution of deep blue color and second is leucomethylene blue (LuMB) form having colorless appearance (Asmare et al., 2022). Optimum conditions were used for the catalytic degradation of MB and Fig. 3d having representative peak for MB at 665 nm disappeared which indicated its degradation up to 95.88% in 16 min (Fig. 3e). It can be concluded that the catalytic degradation has led to the formation of LuMB which is the non-toxic form of the dye MB (Leonard et al., 2011). The degradation of MB with such high percentages and in shorter time interval comprehends the efficiency of Ag-NiO₂@PVA NC.

EY is hydrophilic, anionic dye, which shows green-yellow fluorescence. It is also a heterocyclic dye which contains bromine atoms (Anitha, 2016). It is a tetrabromofluorescein dye which has been used to test the catalytic potential of the synthesized NC. It is obtainable as a disodium salt (ES₂⁻) of orange color and it can be reduced to get ESH₂ form which is pale yellow in color and non-toxic (Moser and Graetzel, 1984, Vignesh et al., 2014). In the current study, the catalytic degradation of EY was recorded in the presence of the NC and reducing agent. It can be seen in Fig. 3g that the deep orange color having peak at λ_{\max} = 510 nm faded gradually and become colorless in 20 min showing the efficiency of the catalyst. The removal percentage of EY dye turned out to be 96.56% (Fig. 3h) due to the effectiveness of the Ag-NiO₂@PVA NC (Dsouza et al., 2021).

The model catalytic reactions for all the selected dyes were carried out in our studies and it turned out to be pseudo 1st order kinetics (Fig. 3 c, f, i) followed Langmuir–Hinshelwood mechanism (LHM). In the current study, Ag-NiO₂@PVA have been greater activity against dyestuff as the composite has grander surface area in comparison to the MNPs (Naseem et al., 2022). The rate of reaction can be calculated from the slope of the graph using the mathematical formula of the kinetic model: $\ln(A_t/A_0) = -k_{\text{obs}}x$; where, A₀ show absorbance at zero 't' and A_t appears to be absorbance at any 't'. Observed rate constant (k_{obs}) was obtained from gradient of the plot of $\ln(A_t/A_0)$ versus time by means of the equation which is equal to 0.1 min⁻¹.

3.5.2. Impact of pH on dye degradation

Degradation of the colorants was performed while keeping different pH environments, ranging from 4.2 to 12.3 for MB (Fig. 4 a, b) and 3.4 – 12.5 for MO (Fig. 4 c, d). The catalytic degradation of acidic (MO) and basic (MB) dyes were investigated to optimize the pH to assess the best catalytic performance of the NC in the presence of NaBH₄. It can be seen that the MB dye degraded more rapidly in basic conditions as compared to acidic environment. The possible reason of suppression of catalytic degradation in acidic environment for basic dye is the interaction of H⁺ ions with electron of BH₄ which causes degradation (Yaseen and Scholz, 2019). So, the degradation was possible more efficiently in the basic environment, as 95.88% removal was observed at 8.3 pH and after that there is a decline in the % removal of MB due to the repulsion between OH⁻ ions and electrons.

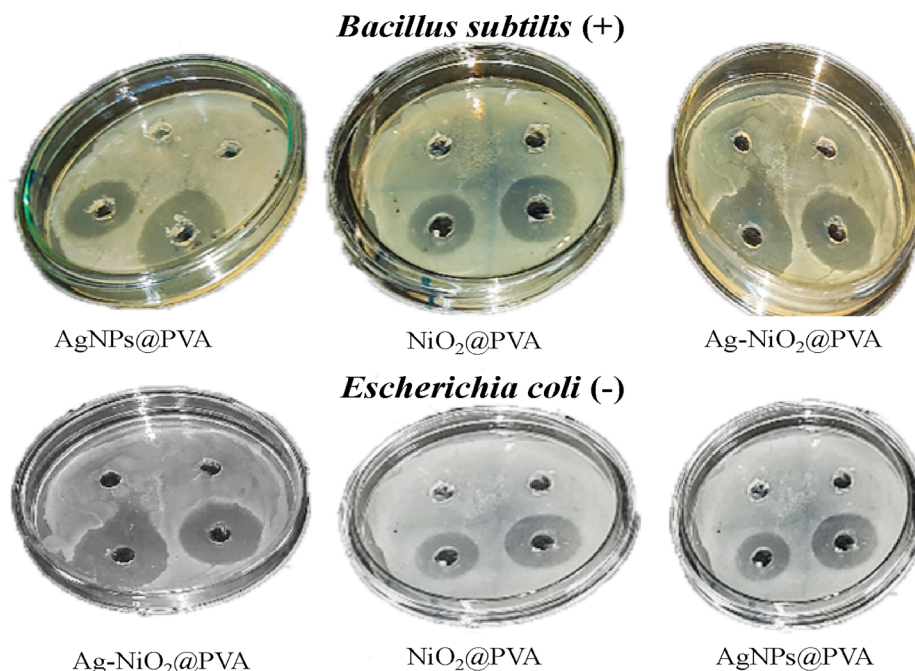


Fig. 8. Comparative antimicrobial activity of synthesized nanocomposite.

On the other hand, acidic dye was degraded in the presence of NC and NaBH_4 in acidic conditions by attaining negative charge (electron) from BH_4^- more effectively due to its attraction with H^+ ions (acidic conditions). The maximum catalytic performance of NC for the degradation of acidic dye (89.26%) was recorded at 3.4 pH (Fig. 4 e, f). Similarly, the same impact of pH has been observed for the catalytic degradation of EY dye in acidic medium due to its anionic character. The % removal for the EY dye degradation was 96.56% at 2.1 pH, which was decreased to 21.99% in highly basic medium due to decrease in electrostatic interaction between COOH^- group of EY dye and catalyst surface (Mishra et al., 2020, Mohapatra and Ghosh, 2023).

3.5.3. Degradation controlled reactions

A comprehensive study has been conceded to ensure catalytic activity of $\text{Ag-NiO}_2@\text{PVA}$ for the removal of selected dyes. For this purpose, the dye degradation reaction was also performed at optimum conditions in the absence of the $\text{Ag-NiO}_2@\text{PVA}$. Fig. 5 (a-f) shows no significant degradation of dyes indicating that only reducing agent cannot instigate the degradation reaction even after 1 h. After adding NC, degradation was observed as it decreases the activation energy of the system vis-à-vis the rate of reaction also increases. Degradation of the selected dyes right after aiding the reaction mixture with the as-synthesized composite as catalysis befalls on the outward of the MNPs which results in the increase in surface area which surely will improve the effectiveness of the catalyst used (Hussain et al., 2021).

The reduction reactions of MB, MO and EY dyes by NaBH_4 in the presence of the NC followed electron transfer process and the possible electron transfer mechanism is demonstrated in Fig. 6. The reducing agent (NaBH_4) release an electron to the surface of the NC ($\text{Ag-NiO}_2@\text{PVA}$) and AZ/AQ dye molecules will be absorbed on the surface of the catalyst. As the NC has the large surface area therefore it acts as a substrate for transfer of electrons (Rajamanikandan et al., 2017). Herein, PVA can act as stabilizing as well as reducing agent, thus preventing particle growth and prevent disturbance in morphology of NC. PVA contains appropriate functional group that can proficiently immobilize NPs and their precursors by van der Waals, electrostatic, dispersive forces or hydrogen/covalent bonds (Sagitha et al., 2016). In many studies, researchers have reported degradation of dyes and organic pollutants by PVA stabilized metal nanoparticles. Comparison of dye degradation potential of nanocomposite with the previous counterpart has been summarized in Table 2.

3.5.4. Stability and reusability

In case of nanocomposite materials, recovery and reusability of the catalyst from the reaction mixture can be the key factor for large scale production and utilization. For the purpose, $\text{Ag-NiO}_2@\text{PVA}$ catalyst was reused up to four consecutive cycles after recovery from MB's model reaction mixture. The graph (Fig. 7a) shows extraordinary results for the reusability of the catalyst $\text{Ag-NiO}_2@\text{PVA}$ and figure demonstrates the percentage activity in terms of MB dye degradation using NC recovered after four consecutive cycles. It endorses that catalyst was not involved as a reactant to reduce MB. Fig. 7b is the FTIR spectra of recycled $\text{Ag-NiO}_2@\text{PVA}$ catalyst, recorded for NC recovered after each cycle. The results of FTIR illustrates minor changes may appear on the surface of nanocomposite and no significant decrease in its efficiency was observed. The results confirmed recycling/ reusability and stability of $\text{Ag-NiO}_2@\text{PVA}$ even after its multiple use for the degradation of selected dye. The results of the current study are well in correlation with the results of previous study (Hussain et al., 2023).

3.5.5. Antibacterial studies

As-synthesis Ag NPs, NiO_2 NP and $\text{Ag-NiO}_2@\text{PVA}$ has displayed great efficiency against different bacterial strains (BS) namely *Bacillus subtilis*, *Staphylococcus aureus* as well as *Escherichia coli* (Table 3 and Fig. 8) and NC exhibited inhibition against all BS. The zone of inhibition of the NC against *S. aureus* is 15.25 mm compared with 7.5 mm of AgNPs and 6.5

mm of NiO_2 NP; lesser zone of inhibition for Ag NPs and NiO NPs were already reported (Ashishie et al., 2018, Kalita et al., 2021). The increased inhibition recorded for NC zone could be due to the synergistic effect of both the metals and PVA against the bacterial strains. As $\text{Ag-NiO}_2@\text{PVA}$ possesses higher surface area to volume ratio therefore it results in the death of the bacterium. It can be interpreted that $\text{Ag-NiO}_2@\text{PVA}$ exhibited antimicrobial potential on both the GP and GN bacteria which means that it not affected by the nature of the bacterial wall (Urnukhsaikhan et al., 2021). Consequently, the nanocomposite has the potential to be used as antimicrobial agent in different medicines or coatings (Singh et al., 2022).

4. Conclusions

Urbanization and industrialization have instigated several environmental problems, especially insufficiency of clean water. Researchers are making enormous efforts for providing hygienic and clean water, besides the management of wastewater. Current research is an effort to gaze for a social and economic addressable cure to eliminate the toxic AZ and AQ dyes which are a major splinter of environmental contamination and to search for materials which can inhibit bacterial growth. We have successfully fabricated PVA-stabilized Ag-NiO_2 NC which are easy to synthesize via low-cost chemical reduction process. Characterization of NC employing state of the art techniques (XRD, FE-SEM and EDAX) confirmed the crystalline nature (hexagonal structure) with an average crystallite size of 9.0145 nm and the particle size of 15.53 nm. Synthesized nanocomposite came up with excellent degradation potential against AZ and AQ organic dyes namely MB, MO and EY. In addition the impact of pH has been studied to achieve maximum degradation efficiency of the nanocomposite. The stability and reusability of the NC has also being studied for four consecutive cycles. Lastly, the synthesized nanocomposites were subjected to antibacterial activity and NC exhibited quite promising results against different bacterial strains. Keeping in view the results of current study, authors would strongly recommend the synthesis of polymer stabilized metal nanocomposite for their possible use as environmental savior. Nanocomposite reported in current study can also be tested for the removal of other organic/inorganic and biological pollutants. In addition, these NC can be used at industrial scale after designing suitable filters for the treatment of wastewater prior discharging to the environment.

CRedit authorship contribution statement

Aimon Saleem: Conceptualization, Supervision. **Amber Iqbal:** . **Umer Younas:** . **Adnan Ashraf:** Formal analysis. **Samiah H. Al-Mijalli:** Project administration, Validation, Funding acquisition. **Faisal Ali:** Methodology. **Muhammad Pervaiz:** . **Zohaib Saeed:** Resources. **Arif Nazir:** . **Munawar Iqbal:** Methodology, Validation.

Funding

This research was funded by Princess Nourah bint Abdulrahman University Researchers Supporting Project number (PNURSP2023R158), Princess Nourah bint Abdulrahman University, Riyadh, Saudi Arabia.

Declaration of competing interest

The authors declare that they have no known competing financial interests or personal relationships that could have appeared to influence the work reported in this paper.

Acknowledgements

The authors express their gratitude to Princess Nourah bint Abdulrahman University Researchers Supporting Project number

(PNURSP2023R158), Princess Nourah bint Abdulrahman University, Riyadh, Saudi Arabia.

References

- Ahlström, L.H., Eskilsson, C.S., Björklund, E., 2005. Determination of banned azo dyes in consumer goods. *TrAC Trends Anal. Chem.* 24, 49–56.
- Ali, F., Younas, U., Nazir, A., et al., 2022. Biosynthesis and characterization of silver nanoparticles using strawberry seed extract and evaluation of their antibacterial and antioxidant activities. *J. Saudi Chem. Soc.* 26, 101558.
- Ali, F., Mehmood, S., Ashraf, A., et al., 2023. Ag–Cu embedded SDS nanoparticles for efficient removal of toxic organic dyes from water medium. *Ind. Eng. Chem. Res.* 62, 4765–4777.
- Anitha, T., 2016. Synthesis of nano-sized chitosan blended polyvinyl alcohol for the removal of Eosin Yellow dye from aqueous solution. *J. Water Process Eng.* 13, 127–136.
- Arif, M., 2023. Catalytic degradation of azo dyes by bimetallic nanoparticles loaded in smart polymer microgels. *RSC Adv.* 13, 3008–3019.
- Arif, M., Farooqi, Z.H., Irfan, A., et al., 2021. Gold nanoparticles and polymer microgels: Last five years of their happy and successful marriage. *J. Mol. Liq.* 336, 116270.
- Ashishie, P.B., Anyama, C.A., Ayi, A.A., et al., 2018. Green synthesis of silver monometallic and copper-silver bimetallic nanoparticles using *Kigelia africana* fruit extract and evaluation of their antimicrobial activities. *Int. J. Phys. Sci.* 13, 24–32.
- Asmare, Z.G., Aragaw, B.A., Atlabachew, M., et al., 2022. Kaolin-supported silver nanoparticles as an effective catalyst for the removal of Methylene Blue Dye from aqueous solutions. *ACS Omega* 8, 480–491.
- Bakar, N.A., Bettahar, M., Bakar, M.A., et al., 2009. Silica supported Pt/Ni alloys prepared via co-precipitation method. *J. Mol. Catal. A: Chem.* 308, 87–95.
- Baz, S., Ikram, M., Haider, A., et al., 2023. Facile synthesis of vanadium oxide/carbon spheres-doped nickel oxide functioned as a nanocatalyst and bactericidal behavior with molecular docking analysis. *ACS omega* 8, 19474–19485.
- Benkhaya, S., M'rabet, S., El Harfi, A., 2020. Classifications, properties, recent synthesis and applications of azo dyes. *Heliyon* 6, e03271.
- Bhat, S.A., Zafar, F., Mondal, A.H., et al., 2020. Photocatalytic degradation of carcinogenic Congo red dye in aqueous solution, antioxidant activity and bactericidal effect of NiO nanoparticles. *J. Iran. Chem. Soc.* 17, 215–227.
- Bhatia, P., Nath, M., 2022. Ag nanoparticles anchored on NiO octahedrons (Ag/NiO composite): An efficient catalyst for reduction of nitro substituted phenols and colouring dyes. *Chemosphere* 290, 133188.
- Bide, M., 2014. Sustainable dyeing with synthetic dyes. Roadmap to sustainable textiles and clothing: eco-friendly raw Materials, technologies, and processing methods, Roadmap to sustainable textile and clothing, pp. 81–107.
- Bishnoi, S., Kumar, A., Selvaraj, R., 2018. Facile synthesis of magnetic iron oxide nanoparticles using inedible *Cynometra ramiflora* fruit extract waste and their photocatalytic degradation of methylene blue dye. *Mater. Res. Bull.* 97, 121–127.
- Bondesgaard, M., Broge, N.L.N., Mamakhel, A., et al., 2019. General solvothermal synthesis method for complete solubility range bimetallic and high-entropy alloy nanocatalysts. *Adv. Funct. Mater.* 29, 1905933.
- Bouzidi, A., Jilani, W., Yahia, I., et al., 2020. Optical analysis and UV-blocking filter of cadmium iodide-doped polyvinyl alcohol polymeric composite films: synthesis and dielectric properties. *J. Inorg. Organomet. Polym. Mater.* 30, 3940–3952.
- Chung, K.-T., 2016. Azo dyes and human health: A review. *J. Environ. Sci. Health Part C* 34, 233–261.
- Din, M.I., Nabi, A.G., Rani, A., et al., 2018. Single step green synthesis of stable nickel and nickel oxide nanoparticles from *Calotropis gigantea*: Catalytic and antimicrobial potentials. *Environ. Nanotechnol. Monit. Manage.* 9, 29–36.
- Dsouza, A., Shilpa, M., Gurumurthy, S., et al., 2021. CuAg and AuAg bimetallic nanoparticles for catalytic and heat transfer applications. *Clean Techn. Environ. Policy* 23, 2145–2155.
- Gupta, P., Maurya, S., Pandey, N., et al., 2021. Structural, electrical and humidity sensing properties of nano-structured nickel oxide prepared by sol–gel method. *J. Mater. Sci. Mater. Electron.* 32, 3529–3542.
- He, F., Wang, Y., Zhong, M., et al., 2021. Construction of nickel nanoparticles embedded in nitrogen self-doped graphene-like carbon derived from waste grapefruit peel for multifunctional OER, HER, and magnetism investigations. *J. Environ. Chem. Eng.* 9, 106894.
- Heshmatpour, F., Abazari, R., Balalaie, S., 2012. Preparation of monometallic (Pd, Ag) and bimetallic (Pd/Ag, Pd/Ni, Pd/Cu) nanoparticles via reversed micelles and their use in the Heck reaction. *Tetrahedron* 68, 3001–3011.
- Humayun, M., Pi, W., Yuan, Y., et al., 2021. A rational design of g-C₃N₄-based ternary composite for highly efficient H₂ generation and 2, 4-DCP degradation. *J. Colloid Interface Sci.* 599, 484–496.
- Hussain, I., Farooqi, Z.H., Ali, F., et al., 2021. Poly(styrene@ N-isopropylmethacrylamide-co-methacrylic acid)@ Ag hybrid particles with excellent catalytic potential. *J. Mol. Liq.* 335, 116106.
- Hussain, I., Shahid, M., Ali, F., et al., 2023. Polymer hydrogels for stabilization of inorganic nanoparticles and their application in catalysis for degradation of toxic chemicals. *Environ. Technol.* 44, 1679–1689.
- Ichyanagi, Y., Wakabayashi, N., Yamazaki, J., et al., 2003. Magnetic properties of NiO nanoparticles. *Phys. B: Condens. Matter* 329, 862–863.
- Kalita, C., Sarkar, R.D., Verma, V., et al., 2021. Bayesian modeling coherenced green synthesis of NiO nanoparticles using *camellia sinensis* for efficient antimicrobial activity. *BioNanoScience* 11, 825–837.
- Kanchana, S., Vijayalakshmi, R., 2020. Photocatalytic degradation of organic dyes by PEG and PVP capped Cu, Ni and Ag nanoparticles in the presence of NaBH₄ in aqueous medium. *J. Water Environ. Nanotechnol.* 5, 294–306.
- Karunamoorthy, S., Velluchamy, M., 2018. Design and synthesis of bandgap tailored porous Ag/NiO nanocomposite: an effective visible light active photocatalyst for degradation of organic pollutants. *J. Mater. Sci. Mater. Electron.* 29, 20367–20382.
- Kayal, S., Ramanujan, R., 2010. Doxorubicin loaded PVA coated iron oxide nanoparticles for targeted drug delivery. *Mater. Sci. Eng. C* 30, 484–490.
- Khairnar, S.D., Shrivastava, V.S., 2019. Facile synthesis of nickel oxide nanoparticles for the degradation of Methylene blue and Rhodamine B dye: a comparative study. *J. Taibah Univ. Sci.* 13, 1108–1118.
- Khalil, A., Ali, N., Asiri, A.M., et al., 2021. Synthesis and catalytic evaluation of silver@nickel oxide and alginate biopolymer nanocomposite hydrogel beads. *Cellul.* 28, 11299–11313.
- Kooti, M., Jorfi, M., 2009. Synthesis and characterization of nanosized NiO₂ and NiO using Triton® X-100. *Open Chem.* 7, 155–158.
- Lai, C., Huang, F., Zeng, G., et al., 2019. Fabrication of novel magnetic MnFe₂O₄/biochar composite and heterogeneous photo-Fenton degradation of tetracycline in near neutral pH. *Chemosphere* 224, 910–921.
- Lamayi, W., Shehu, Z., Mai, A.J., et al., 2020. Green synthesis, characterization and larvicidal activity of Cu/Ni bimetallic nanoparticles using fruit extract of *Palmyra palm*. *Int. J. Chem. Mater. Res.* 8, 20–25.
- Leonard, K., Ahmmad, B., Okamura, H., et al., 2011. In situ green synthesis of biocompatible ginseng capped gold nanoparticles with remarkable stability. *Colloids Surf. B: Biointerfaces* 82, 391–396.
- Li, G.-J., Kawi, S., 1998. Synthesis, characterization and sensing application of novel semiconductor oxides. *Talanta* 45, 759–766.
- Li, C., Zhou, K., Qin, W., et al., 2019. A review on heavy metals contamination in soil: effects, sources, and remediation techniques. *Soil Sediment Contam. Int. J.* 28, 380–394.
- Liu, W., Fan, C., Zong, Z., et al., 2020. Two Co (II)-based metal organic frameworks for highly efficient removal of azo dyes from aqueous environment: Synthesis, selective adsorption and adsorption mechanism. *Colloids Surf. A Physicochem. Eng. Asp.* 603, 125236.
- Liu, J., Li, X., Zeng, X., 2010. Silver nanoparticles prepared by chemical reduction-protection method, and their application in electrically conductive silver nanopaste. *J. Alloy. Compd.* 494, 84–87.
- Mahmoud, K., 2015. Synthesis, characterization, optical and antimicrobial studies of polyvinyl alcohol–silver nanocomposites. *Spectrochim. Acta Part A: Mol. Biomol. Spectrosc.* 138, 434–440.
- Mallampati, R., Valiyaveetil, S., 2014. Eggshell membrane-supported recyclable catalytic noble metal nanoparticles for organic reactions. *ACS Sustain. Chem. Eng.* 2, 855–859.
- Manzoor, J. and M. Sharma, 2020. Impact of textile dyes on human health and environment. Impact of textile dyes on public health and the environment, IGI Global: 162–169.
- Mishra, S., M. Priyadarshinee, A. Debnath, et al., 2020. Rapid microwave assisted hydrothermal synthesis cerium vanadate nanoparticle and its photocatalytic and antibacterial studies. 137, 109211.
- Mohammed, W., Matalkeh, M., Al Soubaihi, R.M., et al., 2023. Visible Light Photocatalytic Degradation of Methylene Blue Dye and Pharmaceutical Wastes over Ternary NiO/Ag/TiO₂ Heterojunction. *ACS omega* 8, 40063–40077.
- Mohapatra, T. and P. J. C. P. Ghosh, 2023. Fenton-like oxidation of Eosin Yellow using laterite catalyst in a circulating fluidized-bed reactor: optimization, kinetics, and mass transfer study. 77, 6285–6297.
- Mokoena, T.P., Swart, H.C., Motaung, D.E., 2019. A review on recent progress of p-type nickel oxide based gas sensors: Future perspectives. *J. Alloy. Compd.* 805, 267–294.
- Moser, J., Graetzel, M., 1984. Photosensitized electron injection in colloidal semiconductors. *J. Am. Chem. Soc.* 106, 6557–6564.
- Moustakas, M., 2021. The role of metal ions in biology. *biochemistry and medicine* 14, 549.
- Mrunal, V.K., Vishnu, A.K., Momin, N., et al., 2019. Cu₂O nanoparticles for adsorption and photocatalytic degradation of methylene blue dye from aqueous medium. *Environ. Nanotechnol. Monit. Manage.* 12, 100265.
- Muenze, R., Hannemann, C., Orlinkiy, P., et al., 2017. Pesticides from wastewater treatment plant effluents affect invertebrate communities. *Sci. Total Environ.* 599, 387–399.
- Naseem, K., Ali, F., Tahir, M.H., et al., 2022. Investigation of catalytic potential of sodium dodecyl sulfate stabilized silver nanoparticles for the degradation of methyl orange dye. *J. Mol. Struct.* 1262, 132996.
- Nitu, S., Milea, M.S., Boran, S., et al., 2022. Experimental and computational study of novel pyrazole azo dyes as colored materials for light color paints. *Materials* 15, 5507.
- Noureen, L., Xie, Z., Hussain, M., et al., 2021. BiVO₄ and reduced graphene oxide composite hydrogels for solar-driven steam generation and decontamination of polluted water. *Sol. Energy Mater. Sol. Cells* 222, 110952.
- Ould-Ely, T., Thurston, J.H., Kumar, A., et al., 2005. Wet-chemistry synthesis of nickel–Bismuth bimetallic nanoparticles and nanowires. *Chem. Mater.* 17, 4750–4754.
- Piella, J., Merkoçi, F., Genç, A., et al., 2017. Probing the surface reactivity of nanocrystals by the catalytic degradation of organic dyes: the effect of size, surface chemistry and composition. *J. Mater. Chem. A* 5, 11917–11929.
- Puvaneswari, N., J. Muthukrishnan and P. Gunasekaran, 2006. Toxicity assessment and microbial degradation of azo dyes.
- Rajamanikandan, R., Shanmugaraj, K., Ilanchelian, M., 2017. Concentration dependent catalytic activity of glutathione coated silver nanoparticles for the reduction of 4-nitrophenol and organic dyes. *J. Clust. Sci.* 28, 1009–1023.

- Rashad, M., 2020. Tuning optical properties of polyvinyl alcohol doped with different metal oxide nanoparticles. *Opt. Mater.* 105, 109857.
- Sabzehparvar, M., Kiani, F., Tabrizi, N.S., 2021. Mesoporous-assembled TiO₂-NiO-Ag nanocomposites with pn/Schottky heterojunctions for enhanced photocatalytic performance. *J. Alloy. Compd.* 876, 160133.
- Sachi, A. P. Singh and M. Thirumal, 2021. Fabrication of AgNi Nano-alloy-Decorated ZnO Nanocomposites as an Efficient and Novel Hybrid Catalyst to Degrade Noxious Organic Pollutants. *ACS omega.* 6, 34771-34782.
- Safajou, H., Khojasteh, H., Salavati-Niasari, M., et al., 2017. Enhanced photocatalytic degradation of dyes over graphene/Pd/TiO₂ nanocomposites: TiO₂ nanowires versus TiO₂ nanoparticles. *J. Colloid Interface Sci.* 498, 423-432.
- Sagitha, P., Sarada, K., Muraleedharan, K., 2016. One-pot synthesis of poly vinyl alcohol (PVA) supported silver nanoparticles and its efficiency in catalytic reduction of methylene blue. *Trans. Nonferrous Metals Soc. China* 26, 2693-2700.
- Sarkar, S., Banerjee, A., Halder, U., et al., 2017. Degradation of synthetic azo dyes of textile industry: a sustainable approach using microbial enzymes. *Water Conserv. Sci. Eng.* 2, 121-131.
- Shaheen, K., Suo, H., Shah, Z., et al., 2020. Ag-Ni and Al-Ni nanoparticles for resistive response of humidity and photocatalytic degradation of Methyl Orange dye. *Mater. Chem. Phys.* 244, 122748.
- Shahid, M., Farooqi, Z.H., Begum, R., et al., 2020. Hybrid microgels for catalytic and photocatalytic removal of nitroarenes and organic dyes from aqueous medium: a review. *Crit. Rev. Anal. Chem.* 50, 513-537.
- Shahid, M., Farooqi, Z.H., Begum, R., et al., 2022. Multi-functional organic-inorganic hydrogel microspheres as efficient catalytic system for reduction of toxic dyes in aqueous medium. *Z. Phys. Chem.* 236, 87-105.
- Shen, L., Zhou, X., Wang, A., et al., 2017. Hydrothermal conversion of high-concentrated glycerol to lactic acid catalyzed by bimetallic CuAu_x (x= 0.01-0.04) nanoparticles and their reaction kinetics. *RSC Adv.* 7, 30725-30739.
- Shindy, H., 2017. Fundamentals in the chemistry of cyanine dyes: A review. *Dyes Pigm.* 145, 505-513.
- Shoair, A.G.F., Shanab, M.M., El-Ghamaz, N.A., et al., 2023. Green catalytic conversion of some benzylic alcohols to acids by NiO₂ nanoparticles (NPNPs) in water. *Catalysts* 13, 645.
- Shultz, L.R., Hu, L., Preradovic, K., et al., 2019. A broader-scope analysis of the catalytic reduction of nitrophenols and azo dyes with noble metal nanoparticles. *ChemCatChem* 11, 2590-2595.
- Singh, I., Mazhar, T., Shrivastava, V., et al., 2022. Bio-assisted synthesis of bi-metallic (Ag-Zn) nanoparticles by leaf extract of *Azadirachta indica* and its antimicrobial properties. *Int. J. Nano Dimension* 13, 168-178.
- Singh, P., Mukherjee, A., Mahato, A., et al., 2022. A review on chemoselective reduction of nitroarenes for wastewater remediation using biochar supported metal catalysts: Kinetic and mechanistic studies. *Chem. Afr.* 1-18.
- Song, T., Gao, F., Guo, S., et al., 2021. A review of the role and mechanism of surfactants in the morphology control of metal nanoparticles. *Nanoscale* 13, 3895-3910.
- Sun, Y., Liao, Y., Chen, X., et al., 2022. Scalable synthesis of reusable Ag@ NiO micro-nanosynergized composite for highly fast reduction of 4-nitrophenol. *J. Nanopart. Res.* 24, 238.
- Tang, S., Zheng, J., 2018. Antibacterial activity of silver nanoparticles: structural effects. *Adv. Healthc. Mater.* 7, 1701503.
- Teoh, L.G., Li, K.-D., 2012. Synthesis and characterization of NiO nanoparticles by sol-gel method. *Mater. Trans.* 53, 2135-2140.
- Tokiwa, H., Ohnishi, Y., Rosenkranz, H.S., 1986. Mutagenicity and carcinogenicity of nitroarenes and their sources in the environment. *CRC Crit. Rev. Toxicol.* 17, 23-58.
- Ullah, R., Khitab, F., Gul, H., et al., 2023. Superparamagnetic zinc ferrite nanoparticles as visible-light active photocatalyst for efficient degradation of selected textile dye in water. *Catalysts* 13, 1061.
- Urnukhsaikhan, E., Bold, B.E., Gunbileg, A., et al., 2021. Antibacterial activity and characteristics of silver nanoparticles biosynthesized from *Carduus crispus*. *Sci. Rep.* 11, 21047.
- Vacchi, F.I., de Souza Vendemiatti, J.A., da Silva, B.F., et al., 2017. Quantifying the contribution of dyes to the mutagenicity of waters under the influence of textile activities. *Sci. Total Environ.* 601, 230-236.
- Vignesh, K., Priyanka, R., Hariharan, R., et al., 2014. Fabrication of CdS and CuWO₄ modified TiO₂ nanoparticles and its photocatalytic activity under visible light irradiation. *J. Ind. Eng. Chem.* 20, 435-443.
- Wang, N., Feng, Y., Zheng, Y., et al., 2021. New hydrogen bonding enhanced polyvinyl alcohol based self-charged medical mask with superior charge retention and moisture resistance performances. *Adv. Funct. Mater.* 31, 2009172.
- Wojtaszek, K., Cebula, F., Rutkowski, B., et al., 2023. Synthesis and catalytic study of NiAg bimetallic core-shell nanoparticles. *Materials* 16, 659.
- Xie, S., Huang, P., Kruzic, J.J., et al., 2016. A highly efficient degradation mechanism of methyl orange using Fe-based metallic glass powders. *Sci. Rep.* 6, 21947.
- Yaseen, D.A., Scholz, M., 2019. Impact of pH on the treatment of artificial textile wastewater containing azo dyes using pond systems. *Int. J. Environ. Res.* 13, 367-385.
- Yu, Y., Luan, D., Bi, C., et al., 2018. Synthesis of polystyrene microsphere-supported Ag-Ni alloyed catalysts with core-shell structures for electrocatalytic performance. *Polym.-Plast. Technol. Eng.* 57, 875-883.